

Tight-Binding Calculation of Ti-Rh-Type Phase Diagram

M. Sluiter, P. Turchi,^(a) Fu Zezhong,^(b) and D. de Fontaine

*Department of Materials Science and Mineral Engineering and Lawrence Berkeley Laboratory,
University of California, Berkeley, California 94720*

(Received 1 June 1987)

Tight-binding electronic band-structure calculations were combined with a free-energy expression from a statistical mechanical method called the cluster-variation method. The effective pair interactions used in the cluster-variation calculation were evaluated by the generalized perturbation method. Only d orbitals were included and the numbers of d electrons per atom were taken to be three for the pure A element and eight for the pure B . A phase diagram was constructed incorporating, for the first time, both fcc and bcc lattices and their simple-ordered superstructures. The calculated diagram agreed reasonably well with those determined empirically for Ti-Rh or Ti-Ir.

PACS numbers: 61.55.Hg, 64.60.Cn, 64.75.+g, 71.20.Cf

The task of calculating alloy phase diagrams from first principles is both practical and challenging: practical because the study of alloy properties depends critically on the knowledge of the relevant phase diagrams, challenging because the necessary calculations must combine, at a high level of accuracy, both quantum mechanical and statistical thermodynamical contributions. Recently, electronic band-structure calculations have been used, in conjunction with appropriate statistical mechanical models, to derive portions of phase diagrams virtually from first principles. Recent examples include the calculation of the Cr-Mo miscibility gap¹ and of important features of binary semiconductor systems.² The purpose of this note is to present the results of a calculation of the phase diagram of a transition-metal binary alloy exhibiting both fcc and bcc solid solutions and ordered intermetallic compounds. The prototype system chosen was Ti-Rh (or Ti-Ir).

The computational scheme employed is summarized briefly below. Details of the calculations will be given elsewhere.^{3,4} Starting assumptions are that atoms of two types, A and B , occupy the sites of either a bcc or fcc lattice with constant lattice parameter. No displacements, either static (elastic) or dynamic (vibrational) are allowed. It is further assumed that, for the transition elements considered, ferromagnetic ones excluded, only d electrons are responsible for bonding. The band structure is calculated in a tight-binding (TB) scheme featuring canonical Slater-Koster parameters⁵: $dd\pi = \frac{1}{2} |dd\sigma|$, $dd\delta = 0$, $dd\sigma = -1.385$. For the fcc electronic density of states, these values give a d -band width of 11.08 in canonical units (c.u.), with 1 c.u. \approx 4.5 eV/atom for a typical d -band width of 5 eV. The bcc second nearest-neighbor Slater-Koster parameters were calculated with the assumption of an inverse-fifth-power decay. The only element-specific parameters to enter the calculations are thus the number of d electrons for element A (N_A) and for element B (N_B), and the diagonal disorder δ_d which is defined as the positive difference of

the atomic levels of A and B over the average half bandwidth. Since identical canonical Slater-Koster parameters are used for all elements, no nondiagonal disorder is present. Charge transfer is not taken into account. Since differences of energy between ordered and disordered states are required, only band-structure energy terms will be considered, under the assumption that double counting and electrostatic terms will cancel approximately. Although the resulting one-electron TB canonical band model without s - and p -electron contributions yields the correct structural trend from hcp to bcc to hcp to fcc, it cannot be expected to yield the correct structure for each particular element across the transition-metal series.⁶

The statistical mechanical model employed is the

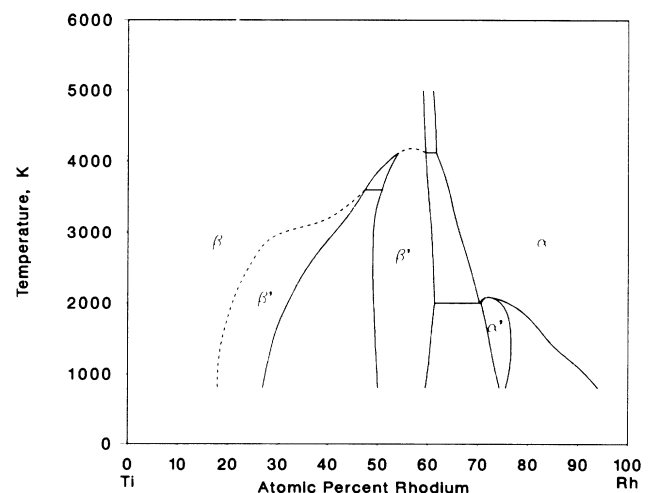


FIG. 1. Calculated phase diagram for Ti-Rh-like binary systems. The miscibility gap between fcc and bcc disordered phases persists to infinite temperatures (in the absence of melting). Phases are α =fcc disordered solid solution (Rh), α' = $L1_2$ (TiRh₃), β =bcc disordered solid solution (Ti), β' = $B2$ (TiRh).

cluster-variation method (CVM)⁷ in the tetrahedron approximation: nearest-neighbor (nn) regular tetrahedron for fcc, and irregular tetrahedron for bcc, comprising nearest- and next-nearest-neighbor (nnn) lattice vectors. The CVM requires, as input, the energy of the completely disordered states U_0^Φ for both lattices [$\Phi = \alpha(\text{fcc})$, $\Phi = \beta(\text{bcc})$], representing the infinite-temperature state frozen in at absolute zero. The quantity $U_0^\Phi(c)$, a function of the atomic concentration of B ($c = c_B$), is evaluated in the single-site coherent potential approximation (CPA).⁸ The required Green's functions are calculated by the recursion method.^{5,9} The CVM further requires, at the very least, in the tetrahedron approximation used here, nn effective pair interactions V_1^α in the fcc case, and $V_1^\beta(\text{nn})$, $V_2^\beta(\text{nnn})$ effective pair interactions in the bcc case. These concentration-dependent interactions are obtained by the generalized perturbation method (GPM) of Ducastelle and Gautier.¹⁰ Relevant formulas are given elsewhere.^{3,5}

Minimization of the CVM free energy must be performed for the disordered phases and also for various expected ordered superstructures of the parent lattices. Ordered superstructures of fcc are designated as α' , α'' , ...; superstructures of bcc are designated as β' ,

β'' , ... For the scheme of pair interactions used here, the ground states of order (superstructures) are fully known^{11,12}: the $L1_2$ (Cu_3Au prototype) and $L1_0$ (CuAu I prototype) structures are possible candidates for fcc, and the $B2$ (CsCl), $B32$ (NaTi), and DO_3 (Fe_3Al) structures for bcc.

Phase diagrams (AB) were calculated for $N_A = 3-5$ and $N_B = 7-9$ d electrons per atom and for diagonal disorder values $\delta_d = 0.6, 0.8$, and 1.0 . Here, only the case $N_A = 3$, $N_B = 8$ will be examined. The reason for that particular choice is as follows: Recent LMTO electronic band-structure calculations¹³ have shown that across the transition-metal series, the number of s electrons in elemental crystals remains approximately constant at about 1.3. Hence, the case (3,8) corresponds roughly to a binary alloy with $A = \text{Ti}$, Zr , or Hf , and $B = \text{Rh}$ or Ir (the ferromagnetic Co element being excluded). Ordering maps based on a rectangular density-of-states model¹⁴ show that such binaries should display ordering tendencies over the whole concentration range, making these systems particularly interesting to study by the CVM. Only for the (3,8) combination does the simple TB approximation used here predict bcc stability for pure A and fcc for pure B . The value $\delta_d = 0.8$ was

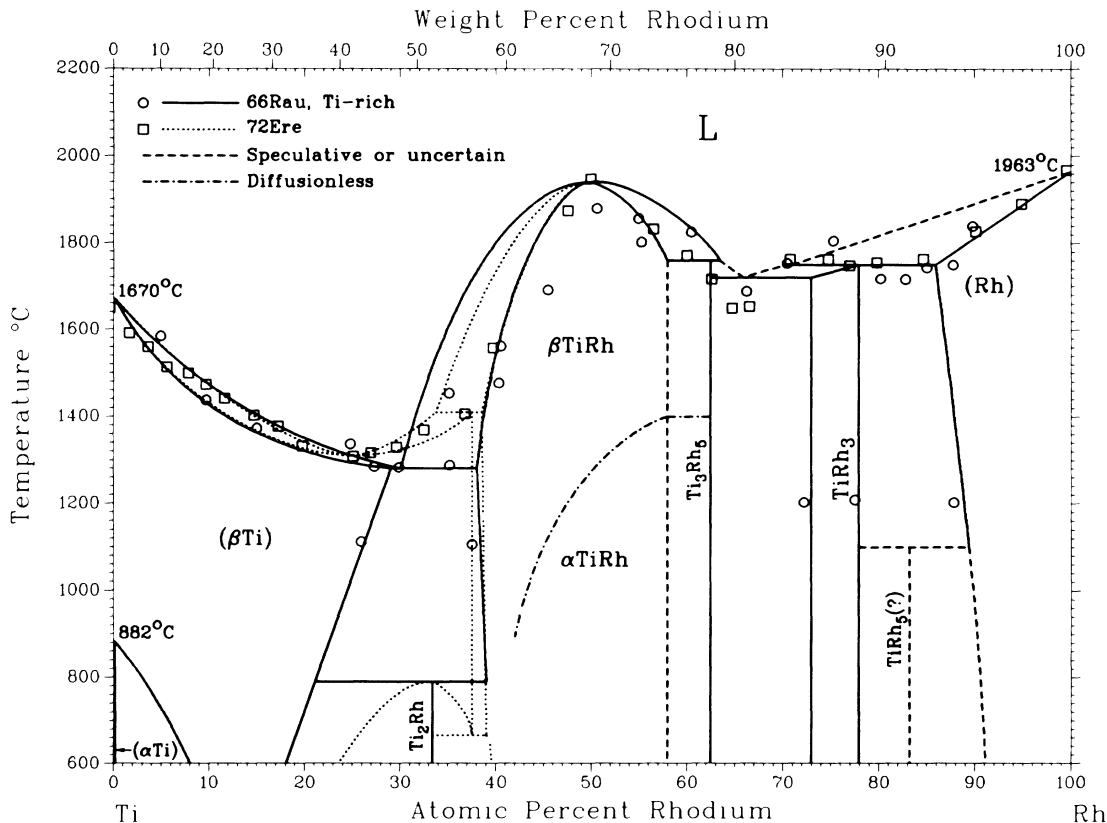


FIG. 2. Assessed Ti-Rh phase diagram according to Ref. 15. βTi corresponds to β used in Figs. 1 and 3, $\beta\text{TiRh} = \beta'$, $\alpha\text{TiRh} = \alpha''$, $\text{TiRh}_3 = \alpha'$; L indicates the liquid.

selected because the calculated phase diagram appeared to agree more closely with the experimentally determined systems than did those obtained with $\delta_d=0.6$ or 1.0.

When the TB-CPA-GPM-CVM computations described briefly above were carried out with the selected parameters, the resulting $U_0(c)$ curves for both fcc and bcc disordered solid solutions had the expected shapes^{3,5} and so did the $V_1^f(c)$ curve (nn effective pair interaction for fcc as a function of concentration). For bcc, the values of V_1^f and V_2^f varied strongly as a function of c , probably as a consequence of our performing the GPM calculation only at lowest order in the pair interactions. Nevertheless, the ratio V_2^f/V_1^f remained at values located between 0 and $\frac{2}{3}$, thereby guaranteeing relative stability of the $B2$ over the $B32$ superstructure.¹²

When free energies of both fcc and bcc disordered and ordered phases were combined, the diagram of Fig. 1 was obtained. It is apparent that phase equilibria are dominated on the A (Ti) side by the bcc lattice, on the B (Rh) side, by the fcc lattice. The fcc + bcc ($\alpha + \beta$) two-phase region located at about 60% B must necessarily persist to infinite temperatures. In the center of the phase diagram, the $B2$ phase (bcc superstructure) overwhelms the $L1_0$ (fcc superstructure) for geometrical reasons: for dominant nn pair interaction, ordering is optimized in the bcc lattice ($B2$ ordered structure), whereas it is frustrated in the fcc lattice, the characteristic feature of that lattice being the equilateral nn triangle for which only AAB or ABB partial order can be achieved. The ordered $B2$ (β') phase is found in two regions of the diagram: somewhat off center (50% to 60% B) and way off stoichiometry. That latter feature may well be an artifact of the type of approximation used here for the calculation of nn and nnn bcc pair interactions. Second-order transitions (dashed lines), allowed by the Landau rules, are predicted at the top of the central $B2$ region and between the disordered β and the strongly off stoichiometric β' . The α' superstructure ($L1_2$), located at about A_3B is separated from the parent disordered fcc (α) by first-order transitions, as expected. The locus of equality between the $B2$ and metastable $L1_0$ phases has also been plotted as a dashed curve in Fig. 3. The temperature scale was fixed by adoption of the canonical d -band width of 5 eV.

Available experimental data on the Ti-Rh and Ti-Ir systems have been examined recently by Murray¹⁵ and the resulting "assessed" phase diagram for Ti-Rh is shown in Fig. 2. Empirically determined phase diagrams for Ti-Ir, Zr-Rh, and Zr-Ir are quite similar in their essential features. At first glance, theoretically (Fig. 1) and experimentally determined (Fig. 2) phase diagrams seem to differ significantly. It must be recognized, however, that the scope of the present computation is a limited one: Only the two basic lattices, fcc and bcc, were considered along with their allowed superstructures; i.e.,

a total of eleven possible phases were entered into the calculation. Out of these, the minimization procedure correctly predicts, at approximately correct location, the following: the β Ti phase, the β TiRh (β' in Fig. 1, correct $B2$ structure), and the TiRh₃ (α' in Fig. 1, correct $L1_2$ structure). The region marked " α TiRh" on the experimentally determined phase diagram (Fig. 2) is separated from β TiRh by a dot-dashed curve which pertains to a diffusionless transformation. It is known that α TiRh is a metastable phase, of uncertain crystal structure, but described generally as "distorted $L1_0$."

Experimentally observed, but imperfectly characterized phases, Ti₂Rh (Laves phase), Ti₃Rh₅, and TiRh₅ could not be predicted by the present model since these phases have crystal structures not contained in the set of possible superstructures of fcc or bcc, and were therefore not included in the calculation.

The most flagrant shortcoming of the calculated diagram is, of course, the absence of liquid-phase equilibria. Here, for the sake of illustration, we constructed an empirical liquid free-energy function, based on a subregular solution model¹⁶ the parameters of which were fitted⁴ to provide the correct pure Ti and pure Rh melting temperatures and the β TiRh congruent melting temperature. Experimentally determined¹⁷ values of Ti and Rh entropies of melting were included. The fitted free energy was then combined with calculated crystalline phase free energies to produce the phase diagram of Fig. 3. The agreement between theory and experiment is now much more striking.

In conclusion, we have shown that, with a canonical TB scheme, it was possible to calculate a reasonable phase diagram for the Ti-Rh (or Ti-Ir) system. More importantly, we have shown that stable and metastable phase equilibria in this class of binary systems can be un-

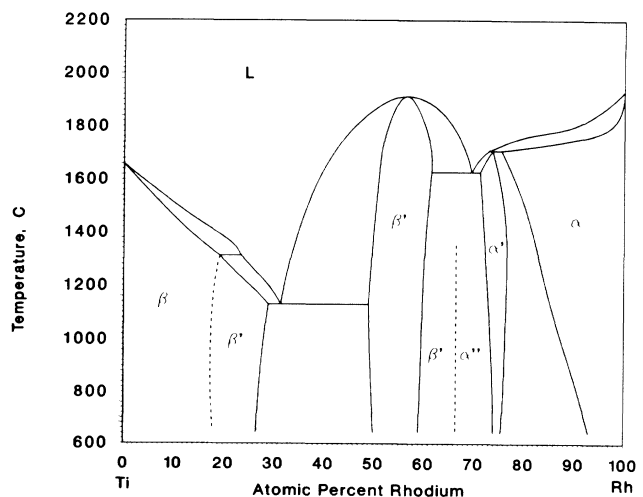


FIG. 3. Phase diagram calculated as in Fig. 1 but with fitted free-energy curve for the liquid phase included. Phases are $\alpha'' = L1_0$ (TiRh), $L =$ liquid; other phases as in Fig. 1.

derstood on the basis of competition between fcc and bcc solid solution tendencies, each lattice contributing its own set of candidate ordered superstructures. The model is currently being improved upon and will be tested on other systems.

The work of M. Sluiter and P. Turchi was supported by a grant from the Lawrence Livermore National Laboratory, M. Fluss, principal investigator. The research was supported in part, at the Lawrence Berkeley Laboratory, by the Director, Office of Energy Research, Materials Sciences Division, U.S. Department of Energy, under Contract No. DE-AC03-76SF00098. The authors thank J. L. Murray for having supplied them with a copy of Ref. 15 prior to publication, and J. B. Clark for supplying them with a copy of Fig. 2.

^(a)Present address: Department of Materials Science (L 280), Lawrence Livermore National Laboratory, P.O. Box 808, Livermore, CA 94550.

^(b)Permanent address: Department of Materials Science MS 138-78, Keck Laboratory, California Institute of Technology, Pasadena, CA 91125.

¹C. Sigli, M. Kosugi, and J. M. Sanchez, Phys. Rev. Lett. **57**, 253 (1986).

²A. A. Mbaye, L. G. Ferreira, and A. Zunger, Phys. Rev. Lett. **58**, 49 (1987).

³P. Turchi, M. Sluiter, and D. de Fontaine, Phys. Rev. B **36**, 3161 (1987).

⁴M. Sluiter, P. Turchi, Fu Zezhong, and D. de Fontaine, to be published.

⁵P. Turchi, Thèse de Doctorat d'Etat, University of Paris VI, 1984 (unpublished).

⁶H. L. Skriver, Phys. Rev. B **31**, 1909 (1985).

⁷R. Kikuchi, Phys. Rev. **81**, 988 (1951).

⁸B. Velicky, S. Kirkpatrick, and H. Ehrenreich, Phys. Rev. **175**, 747 (1968).

⁹R. Haydock, in *Solid State Physics*, edited by H. Ehrenreich, F. Seitz, and D. Turnbull (Academic, New York, 1980), Vol. 35, p. 215.

¹⁰F. Gautier, F. Ducastelle, and J. Giner, Philos. Mag. **31**, 1373 (1975); F. Ducastelle and F. Gautier, J. Phys. F **6**, 2039 (1976).

¹¹J. Kanamori and Y. Kakehashi, J. Phys. (Paris), Colloq. **38**, C7-274 (1977).

¹²S. N. Allen and J. W. Cahn, Acta Metall. **20**, 423 (1972).

¹³O. K. Andersen, O. Jepsen, and D. Glotzel, in *Highlights of Condensed Matter Theory*, International School of Physics, "Enrico Fermi," Course 89, edited by F. Bassani, F. Fermi, and M. P. Tosi (North-Holland, Amsterdam, 1985), p. 59.

¹⁴M. Sluiter, P. Turchi, and D. de Fontaine, J. Phys. C (to be published).

¹⁵J. L. Murray, Bull. Alloy Phase Diagrams **3**, 335 (1982), and to be published.

¹⁶L. Kaufman and H. Bernstein, *Computer Calculation of Phase Diagrams* (Academic, New York, 1970).

¹⁷R. Hultgren, *Thermodynamic Properties of Alloys* (Wiley, New York, 1963).